THIRTEENTH EUROPEAN ROTORCRAFT FORUM

215
Paper No. 58

TOWARD A UNIFIED REPRESENTATION OF ROTOR BLADE AIRLOADS WITH EMPHASIS ON UNSTEADY AND VISCOUS EFFECTS

U. Leiss, S. Wagner

Universität der Bundeswehr München

Institut für Luftfahrttechnik und Leichtbau

September 8-11, 1987

ARLES, FRANCE

ASSOCIATION AERONAUTIQUE ET ASTRONAUTIQUE DE FRANCE

TOWARD A UNIFIED REPRESENTATION OF ROTOR BLADE AIRLOADS WITH EMPHASIS ON UNSTEADY AND VISCOUS EFFECTS

U.Leiss, S. Wagner

Universität der Bundeswehr München
Institut für Luftfahrttechnik und Leichtbau

Abstract

Almost every helicopter analysis program needs an extensive rotor blade airload calculation while iterating in the inner loop. Manifold progress has been achieved to calculate special aerodynamic effects, but no generalized blade element or blade theory exists for the daily practical application in various rotary wing fields. A new method was developed to correlate all steady aerodynamic coefficients with the velocity components in a blade fixed cartesian coordinate system. The unsteady variations are based on the acceleration components. One rotary and three translatory degrees of freedom of each blade element cause different unsteady mechanism. The idealized circulatory and noncirculatory flow was formulated on theoretical basis. The real flow effects due to compressibility, viscosity and unsteadiness are written in terms of the similarity parameters. It is shown, how the superposition principle enables a simultaneous simulation of different flow regimes. It is possible to choose the appropriate model complexity for a specific application without a change of the structure. The new unified model was validated on the comparison with measurement data, however, there exist no experiments of some effects. In this case, the model is formulated on phenomenological basis.

1. Introduction

Increasing speed and maneuverability of rotary wing aircraft require operating conditions of rotors close to the physical limits due to viscosity, compressibility and unsteadiness. The most elaborative work in a rotorcraft analysis program is to calculate the rotorblade airloads in a very complex flow field. Nowadays a CFD calculation for the daily application is still beyond the scope. Consequently an efficient unified representation of rotorblade airloads is a need for almost every rotorcraft disciplin. The arbitrary direction of oncoming flow causes attached and separated flow conditions, which cannot be handled by common aerodynamic formulations.
Therefore, fundamental and simple theoretical results and empirical relations are used simultaneously. The cartesian coordinate system of Fig.1 is introduced, to avoid trigonometric functions.

Aerodynamic forces and moments are based on the dynamic sonic pressure, $q_a = (\rho/2)a^2$:

$$dF_{Ax,y,z} = c_{fx,y,z} \cdot q_a \cdot c \cdot dy$$

$$dM_{Ax,y,z} = c_{mx,y,z} \cdot q_a \cdot c^2 \cdot dy$$

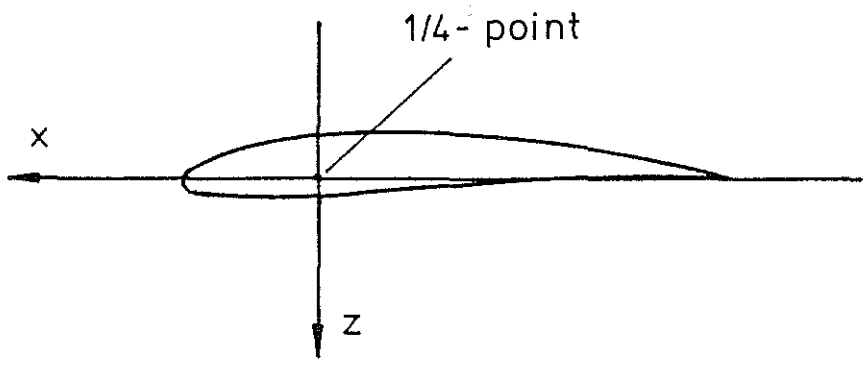

Fig.1: Coordinate system of a blade element

The aerodynamic coefficients are written in terms of velocity and acceleration components as well as the similarity parameters of viscosity, compressibility and unsteadiness (LEISS/WAGNER [3]).
In previous investigations (LEISS [1],[2],[4]) the structure of this new model was presented in the two- and three-dimensional case. Emphasis was placed on the discussions of the choices of typical effects and their formulation. In addition, a comparison between the classic and new form of equations is given to illustrate the new approach. The general purpose of the present work is to present the full fundamental set of superimposed equations for representation of all aerodynamic coefficients.

2. Steady Model

2.1 Idealized Nonviscous Flow

For a long time nonviscous flow was calculated with potential theory including the assumption of small angles of attack. The discontinuous potential theory was used for separated flow, but then rear side pressure is unrealistic. Hypersonic flow is approximately described by the Newton law. The existing basic theories are shown in Fig.2

The present new formulation is based on these fundamental theories with new boundary conditions and applications.
The Newton law is used for all flow regions (LEISS[2]).
The coefficients for a flat plate are:

$$c_{fnx} = 0$$

$$c_{fnz} = 2 \cdot v_z \cdot |v_z| / a^2$$

$$c_{mny} = -0{,}5 \cdot v_z \cdot |v_z| / a^2$$

The approximate extension for arbitrary convex contours is as follows:

$$c_{fnx} \cdot a^2 = (c_{fxx+} + c_{fxx-}) \cdot v_x \cdot |v_x| - (c_{fxz+} + c_{fxz-}) \cdot v_z \cdot |v_z| + (c_{fxx+} - c_{fxx-}) \cdot v_x^2 - (c_{fxz+} - c_{fxz-}) \cdot v_z^2$$

$$c_{fnz} \cdot a^2 = (c_{fzz+} + c_{fzz-}) \cdot v_z \cdot |v_z| + (c_{fzx+} + c_{fzx-}) \cdot v_x \cdot |v_x| + (c_{fzz+} - c_{fzz-}) \cdot v_z^2 + (c_{fzx+} - c_{fzx-}) \cdot v_x^2$$

$$c_{mny} \cdot a^2 = (c_{myx+} - c_{myx-}) \cdot v_x \cdot |v_x| + (c_{myz+} - c_{myz-}) \cdot v_z \cdot |v_z| + (c_{myx+} + c_{myx-}) \cdot v_x^2 + (c_{myz+} + c_{myz-}) \cdot v_z^2$$

The contour coefficients can be precalculated with the differential Newton law.

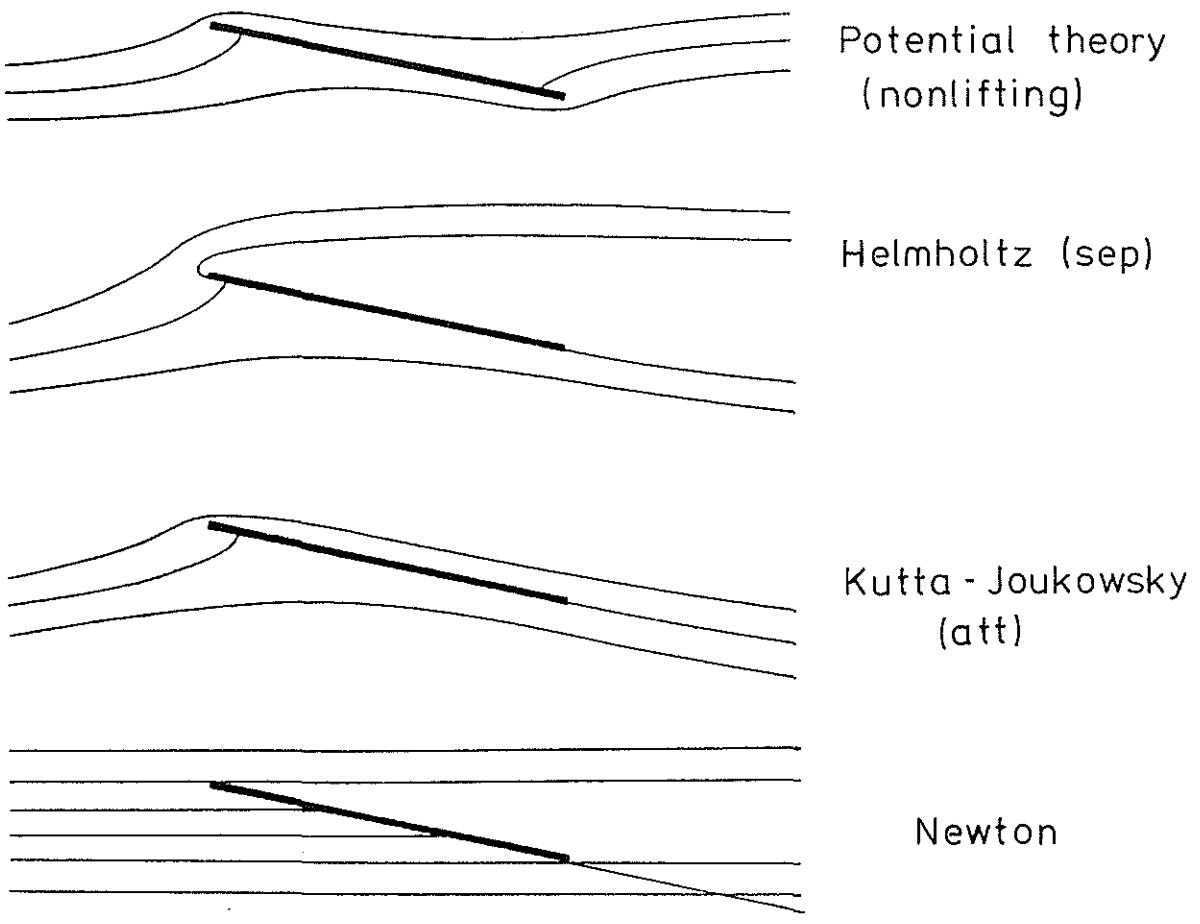

Fig.2: Basic theories for flow around a flat plate

To generalize the aerodynamic loads of a rotor blade, it is necessary to eliminate restrictions for small angles of attack. Therefore, a modified Kutta-condition is used with the result of a new circulation around the profile (LEISS [2]).

$$\Gamma_{new} = \Gamma_{classic} \cdot \cos \alpha$$

The corresponding coefficients for a flat plateare:

$$c_{fxca} \cdot a^2 = -2 \cdot \pi \cdot v_z^2 \cdot v_x / \sqrt{v_x^2 + v_z^2}$$

$$c_{fzca} \cdot a^2 = 2 \cdot \pi \cdot v_z \cdot v_x^2 / \sqrt{v_x^2 + v_z^2}$$

$$c_{myca} \cdot a^2 = 0 \qquad \text{(reference point c/4)}$$

With this condition, the upper boundary for attached circulatory flow is given for arbitrary angles of attack.
Consequently, a lower boundary for separated circulatory flow must be defined. The derivation of the Rayleigh-Kirchhoff theory at small angles of attack was combined with the new Kutta-condition and gives the corresponding coefficients.

$$c_{fxcs} \cdot a^2 = 0 \quad \text{(no suction force)}$$

$$c_{fzcs} \cdot a^2 = 0{,}5 \cdot \pi \cdot v_Z \cdot v_X^2 \,/\, \sqrt{v_X^2 + v_Z^2}$$

$$c_{mycs} \cdot a^2 = -\,(\pi \cdot v_Z \cdot v_X^2)/(\sqrt{v_X^2 + v_Z^2} \cdot 32)$$

It should be noted, that these coefficients are to be superposed on the Newton terms.

2.2 Viscous Effects

Flow around the real profile is viscous. Hence, the aerodynamic coefficients must be within the lower and upper boundary of the corresponding separated and attached idealized flow.

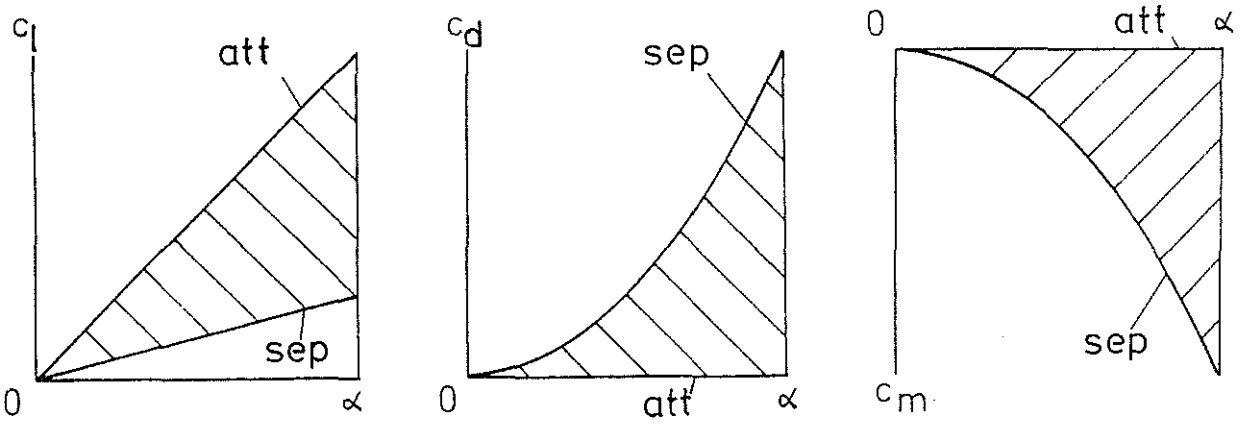

Fig. 3: Regions of viscous flow

Fig.3 shows the typical boundaries of all three aerodynamic coefficients for small angles of attack. The corresponding Reynolds numbers are infinity for the upper and zero for the lower boundary. Technical application needs usually just one specified Reynolds number and a relatively small variation around this working point. The first problem is now to represent the transition curve between the boundaries of Fig.3 for one Reynolds number. At first the lower and upper side of the profile were formulated separately. One circulation function is taken for each side of the profile as indicated in Fig.4.

If, for example, the profile is symmetric, the resultant circulation vanishes at zero angle of attack and has two maxima on both sides of this point. These maximum circulation points are similar to the static stall point, but are unified in their definition, because they have always a maximum due to the superposition on the fully separated flow. The contribution of the attached circulation functions is shown in Fig.5.

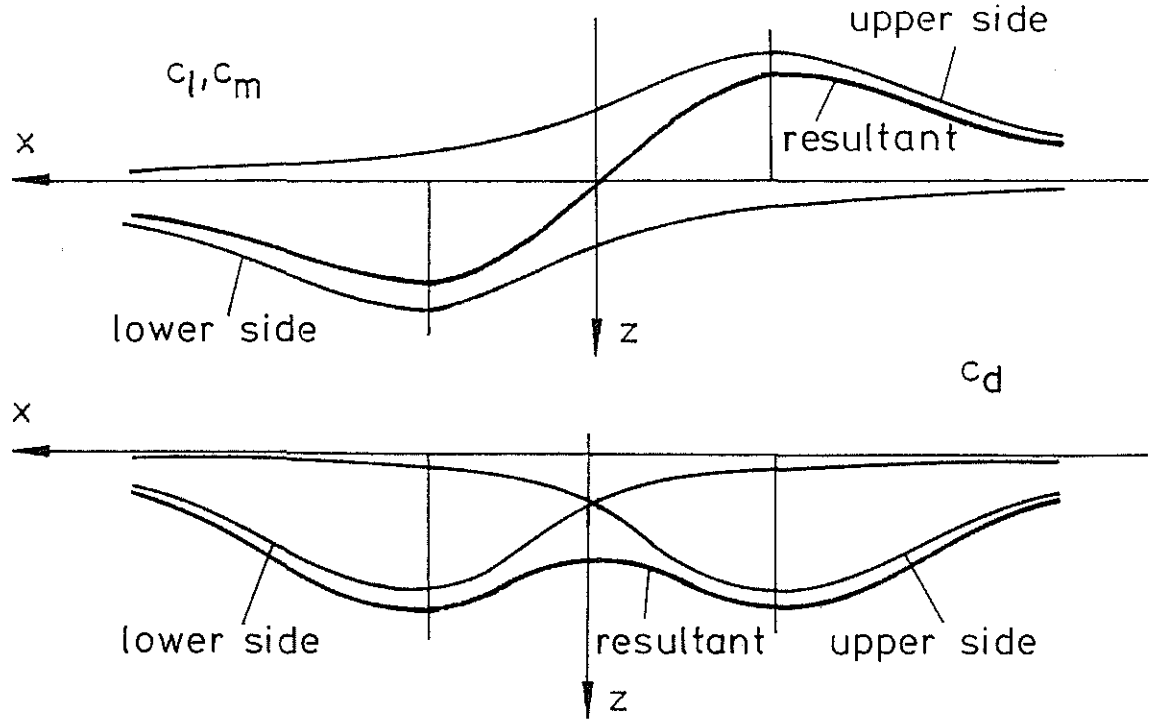

Fig.4: Model of the attached circulatory part of viscous flow

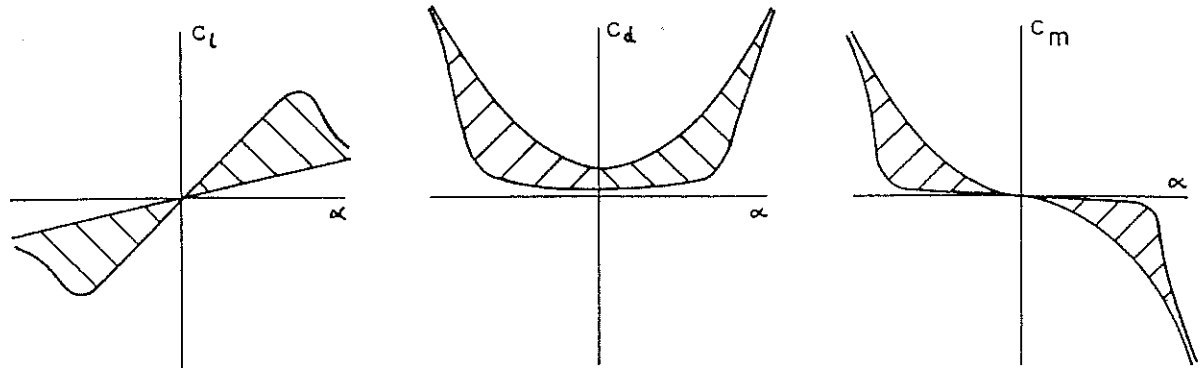

Fig.5: Typical transition from fully attached to fully separated flow

All aerodynamic coefficients are expressed by the same principal structure.

$$\Gamma_{a+} = \frac{c_{ss+}^2}{(v_z - v_{zss+})^2 + c_{ss+}^2} \cdot \frac{d\Gamma_{max+}}{dv_{zss+}} \cdot v_{zss+}$$

$$\Gamma_{a-} = \frac{c_{ss-}^2}{(v_z - v_{zss-})^2 + c_{ss-}^2} \cdot \frac{d\Gamma_{max-}}{dv_{zss-}} \cdot v_{zss-}$$

$$\Gamma_a = \Gamma_{a+} + \Gamma_{a-}$$

The first fractions are the positive and negative circulation functions which are normalized on the maximum unity. The second fractions are the slopes of the maxima. In case of the lift coefficient it is similar to the well-known lift curve slope.
V_{zss} is the normal velocity at the maximum circulation. The choice of these functions including parameters with physical meaning is further the basis to account for different influences on these unique parameters. The earlier mentioned Reynolds number variation about a specified point

can be written:

$$\Delta v_{zss+,-} = c_{Rexss+,-} \left[c \cdot \frac{\nu_{ref}}{c_{ref} \cdot \nu} - 1 \right] + c_{Rezss+,-} \left[t \cdot \frac{\nu_{ref}}{t_{ref} \cdot \nu} - 1 \right]$$

The influence of thickness, chord length and viscosity is included. In addition to the pressure forces, skin friction must be modelled. The superposition principle is realized even in this case. The pure viscous friction is:

$$c_{fxfv} \cdot a^2 = 2 \cdot c_{xfv} \cdot \nu \cdot v_x$$

The laminar boundary layer gives the additional force:

$$c_{fxfl} \cdot a^2 = 2 \cdot c_{xfl} \cdot \sqrt{\frac{\nu}{c}} \cdot v_x \cdot \sqrt{|v_x|}$$

For a flat plate the theoretical coefficient c_{xfl} is 1.328.
The transition from laminar to fully turbulent boundary layer is formulated by

$$c_{fxft} \cdot a^2 = 2 \cdot c_{xft} \frac{Re_x^2}{Re_x^2 + c_{xft50}^2} \cdot v_x^2$$

The total friction force consists of

$$c_{fxf} = c_{fxfv} + c_{fxfl} + c_{fxft}$$

Usually, the theoretical parameters for a flat plate are accurate enough, but can be changed a little for the particular airfoil.

2.3 Effects Of Compressibility

The introduction of Mach number is the second important steady problem. Mach number components are used for the new model.

$$M_x = \frac{v_x}{a} \quad , \quad M_y = \frac{v_y}{a} \quad , \quad M_z = \frac{v_z}{a}$$

All velocity components are replaced by these Mach number components. In addition, the compressible behaviour of the maximum circulation point must be implemented.

$$M_{zss+,-} = M_x \cdot (c_{ss1+,-} + M_x \cdot c_{ss2+,-} + M_x^2 \cdot c_{ss3+,-})$$

Next, the slope of idealized nonviscous flow is divided up into three superimposed flow types to account for arbitrary Mach numbers. First, the subcritical one starts with the theoretical amount of 0.5 π and decreases asymptoticly to zero. The compressible circulatory coefficients in separated flow are:

$$c_{fxcs} = 0$$

$$c_{fzcs} = \frac{\pi}{2} \cdot \frac{c_{cs}^4}{(M_x^2 + M_z^2)^2 + c_{cs}^4} \cdot \frac{M_z \cdot M_x^2}{\sqrt{M_x^2 + M_z^2}}$$

$$c_{mycs} = \frac{\pi}{32} \cdot \frac{c_{cs}^4}{(M_x^2 + M_z^2)^2 + c_{cs}^4} \cdot \frac{M_z \cdot M_x^2}{\sqrt{M_x^2 + M_z^2}}$$

Secondly, the slope of compressible circulation in attached flow increases from 1.5 π with the Prandtl-Glauert rule and breaks down close to sonic speed, dependent on the particular airfoil.

$$\frac{dc_{fx,fy,mzca+,-}}{dM_{zss+,-}} = \frac{c_{ss4+,-} \cdot c_{ss5+,-}^2}{M_x^2 + c_{ss5+,-}^2} + \frac{c_{ss6+,-} \cdot (c_{ss7+,-} - M_x)}{(c_{ss8+,-} - M_x)^2 + c_{ss9+,-}^2}$$

Also the curvature, it means the form of transition from attached to separated flow, is extended.

$$c_{ss+,-} = M_x \cdot (c_{ss10+,-} + M_x \cdot c_{ss11+,-})$$

The complete compressible circulatory coefficients in attached flow are:

$$c_{fxca} = \left[\frac{c_{ssfx+}^2}{(M_z - M_{zssfx+})^2 + c_{ssfx+}^2} \cdot \frac{dc_{fxca+}}{dM_{zssfx+}} \cdot M_{zssfx+} - \frac{c_{ssfx-}^2}{(M_z - M_{zssfx-})^2 + c_{ssfx-}^2} \cdot \frac{dc_{fxca-}}{dM_{zssfx-}} \cdot M_{zssfx-} \right] \cdot |M_x|$$

$$c_{fzca} = \left[\frac{c_{ssfz+}^2}{(M_z - M_{zssfz+})^2 + c_{ssfz+}^2} \cdot \frac{dc_{fzca+}}{dM_{zssfz+}} \cdot M_{zssfz+} + \frac{c_{ssfz-}^2}{(M_z - M_{zssfz-})^2 + c_{ssfz-}^2} \cdot \frac{dc_{fzca-}}{dM_{zssfz-}} \cdot M_{zssfz-} \right] \cdot |M_x|$$

$$c_{myca} = \left[\frac{c_{ssmy+}^2}{(M_z - M_{zssmy+})^2 + c_{ssmy+}^2} \cdot \frac{dc_{myca+}}{dM_{zssmy+}} \cdot M_{zssmy+} + \frac{c_{ssmy-}^2}{(M_z - M_{zssmy-})^2 + c_{ssmy-}^2} \cdot \frac{dc_{myca-}}{dM_{zssmy-}} \cdot M_{zssmy-} \right] \cdot |M_x|$$

For completeness and consistency the transsonic and supersonic slope behaviour is included. It increases from zero at M=0 to a maximum close to M=1 and decreases again asymptoticly to zero, following approximately the Ackeret rule. The corresponding aerodynamic coefficients are

$$c_{fxt} = \frac{c_{t3fx} \cdot M_x \cdot (M_x^2 - c_{t4fx}^2)}{(M_x^2 - c_{t1fx}^2)^2 + c_{t2fx}^4}$$

$$c_{fzt} = 4 \cdot \frac{M_z \cdot M_x^2 (M_x^2 + M_z^2)}{(M_x^2 + M_z^2 - c_{t1fz}^2)^2 + c_{t2fz}^4}$$

$$c_{myt} = \frac{M_z \cdot M_x^2 (M_x^2 + M_z^2)}{(M_x^2 + M_z^2 - c_{t1my}^2)^2 + c_{t2my}^4}$$

Finally, the friction force decreases with increasing Mach number.

$$c_{fxf} = (c_{fxfv} + c_{fxfl} + c_{fxft}) \cdot \frac{c_{fc}^2}{M_x^2 + c_{fc}^2}$$

2.4 Superposition Of Steady Flow

To illustrate the whole concept of superposition of the particular flow types derived so far, Fig.6 shows the behaviour of the force components and the pitching moment as a function of normal Mach number component, which is equivalent to the angle of attack at small amounts.

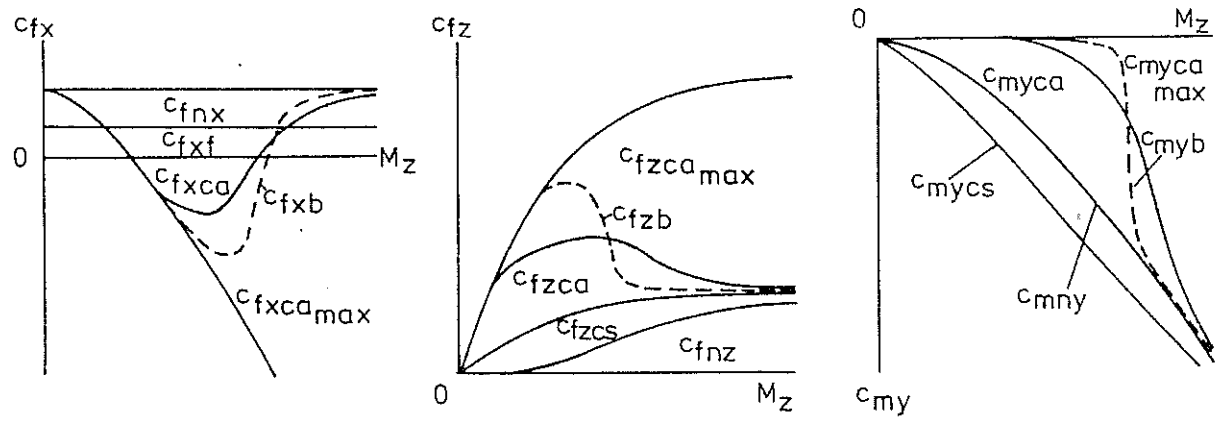

Fig.6: M_Z Superposition

The supplementary M_X dependency indicates Fig.7

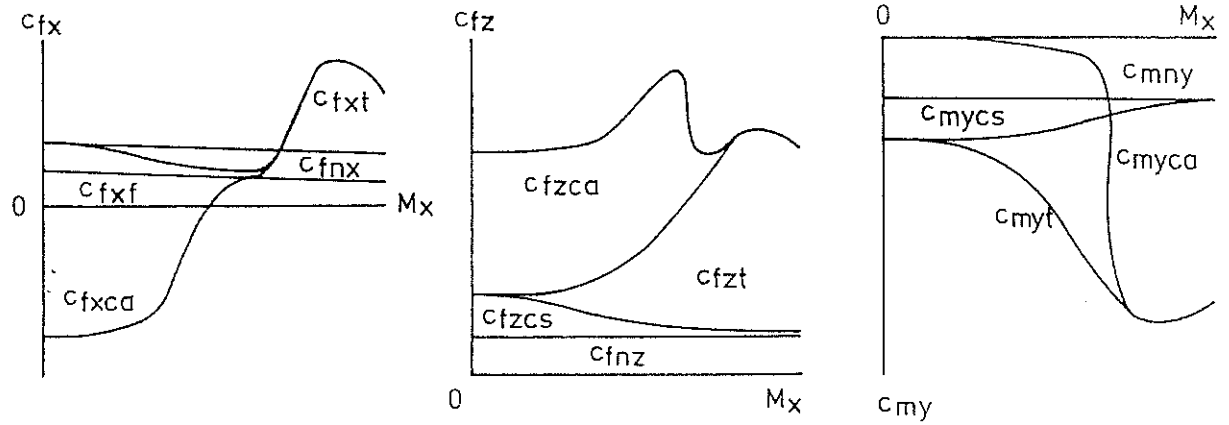

Fig.7: M_X Superposition

The Mach number component is comparable to the resultant one if angles of attack are small. The total steady aerodynamic coefficients are composed of:

$$c_{fx} = c_{fnx} + c_{fxt} + (c_{fxcs}) + c_{fxca} + (c_{fxb}) + c_{fxf}$$

$$c_{fz} = c_{fnz} + c_{fzt} + c_{fzcs} + c_{fzca} + (c_{fzb})$$

$$c_{my} = c_{mny} + c_{myt} + c_{mycs} + c_{myca} + (c_{myb})$$

Terms in parentheses are only for special purposes. The bubble burst

effects can be found in details at LEISS [1].

3. Unsteady Model

To unify physical effects is the most important problem even at unsteady flow conditions. Because of the complexity only few effects can be evaluated theoretically. All other effects must be considered on a phenomenological empirical basis. The derived steady model has unsteady counterparts or consistent extensions of all mechanism and flow types involved. Now, unsteady aerodynamic coefficients can be introduced to all standard rotorcraft analyses on the basis of the present new model without significant increase in man work and computation time.

3.1 Nonviscous Effects

Pure potential theory gives no lift in the steady case, but apparent mass effects in the unsteady one. The apparent mass coefficients for a flat plate are:

$$c_{fxam} = 0$$

$$c_{fzam} = (\dot{\omega}_y \cdot \frac{c}{4} + b_z) \cdot \frac{c \cdot \pi}{2 \cdot a^2}$$

$$c_{myam} = (\dot{\omega}_y \cdot \frac{c \cdot 3}{32} + \frac{b_z}{4}) \cdot \frac{c \cdot \pi}{2 \cdot a^2}$$

The real profile with finite thickness led to an approximate apparent mass term in chord direction:

$$c_{fxam} = b_x \cdot \frac{t \cdot \pi}{2 \cdot a^2} \cdot \frac{t}{c}$$

This term is important for the unsteady drag or tangential force at higher reduced frequency.
The unsteady circulation lag has been derived from WAGNER [5] and KÜSSNER [6] for a step function of the angle of attack or the gust velocity. The exponential approximation of the WAGNER function is

$$W(s) \cong 1 - 0.165 \cdot e^{-0.091 \cdot s} - 0.335 \cdot e^{-0.6 \cdot s}$$

where s is the dimensionsless time in the x-direction

$$s = \frac{v_x \cdot t}{c}$$

The circulation lag due to any arbitrary motion can be evaluated by superposition of an infinite number of steps using the DUHAMEL-integral.

$$dA_c(s) = \pi \cdot \rho \cdot v \cdot c \int_0^s \frac{d}{d\sigma} \cdot v_{z_{3/4}}(\sigma) \cdot w\,(s-\sigma)\, d\sigma \cdot dy$$

Use of normal velocity component instead of the angle of attack led to a clear distinction between the pitch and plunge motion.

$$v_{z_{3/4}} = -\omega \cdot \Delta z \cdot \cos \omega t \qquad \text{(plunge)}$$

$$v_{z_{3/4}} = -\frac{c}{2} \cdot \omega \cdot \Delta\Theta \cdot \cos \omega t \qquad \text{(pitch)}$$

The assumption of harmonic motions enables an analytical solution of the DUHAMEL-integral. The lag of the normal velocity component for pitch motion is:

$$\Delta v_{z_{pitch}} = \frac{c}{2} \cdot \left\{ \dot{\Theta} \cdot -\left[\frac{0.165 \cdot k^2}{0.091^2 + k^2} + \frac{0.335 \cdot k^2}{0.6^2 + k^2} \right] - \ddot{\Theta} \cdot \left[\frac{0.165 \cdot 0.091}{0.091^2 + k^2} + \frac{0.335 \cdot 0.6}{0.6^2 + k^2} \right] \right\}$$

The equivalent correlation for plunge motion is:

$$\Delta v_{z_{plunge}} = \left\{ \dot{z} \cdot \left[\frac{0.165 \cdot k^2}{0.091^2 + k^2} + \frac{0.335 \cdot k^2}{0.6^2 + k^2} \right] - \ddot{z} \cdot \left[\frac{0.165 \cdot 0.091}{0.091^2 + k^2} + \frac{0.335 \cdot 0.6}{0.6^2 + k^2} \right] \right\}$$

Pure unsteady freestream in the present cartesian coordinate system gives no circulation effects, but a circulation lag exists coupled with pitch.

Δv_z pitch-lag-coupling =

$$\left\{ - \left[(v_x - v_{xo}) \cdot \Theta_o + (\Theta - \Theta_o) \cdot v_{xo} \right] \cdot \left[\frac{0.165 \cdot k^2}{0.091^2 + k^2} + \frac{0.335 \cdot k^2}{0.6^2 + k^2} \right] \right.$$

$$- \left[\dot{v}_x \cdot \Theta_o + \dot{\Theta} \cdot v_{xo} \right] \cdot \left[\frac{0.165 \cdot 0.091}{0.091^2 + k^2} + \frac{0.335 \cdot 0.6}{0.6^2 + k^2} \right]$$

$$- \left[(v_x - v_{xo})(\Theta - \Theta_o) \cdot k^2 - \dot{\Theta} \cdot \dot{v}_x \right] \cdot \left[\frac{0.165 \cdot 2}{0.091^2 + 4k^2} + \frac{0.335 \cdot 2}{0.6^2 + 4k^2} \right]$$

$$\left. - \left[\dot{v}_x(\Theta - \Theta_o) + \dot{\Theta}(v_x - v_{xo}) \right] \cdot \left[\frac{0.165 \cdot 0.091}{0.091^2 + 4k^2} + \frac{0.335 \cdot 0.6}{0.6^2 + 4k^2} \right] \right\}$$

So all degrees of freedom were considered in a unified form only based on the WAGNER function. These equations for the circulation lag are valid even in the nonlinear flow regime because of consistency with the extended steady potential theory for arbitrary angles of attack or flow components in the present model.

3.2 Viscous Effects

Unsteady viscous effects are doubtless of great importance for rotorcraft applications. The significant overshoot of lift and the hysteresis of a complete pitch cycle are well known based on a lot of systematic measurements. Empirical and semi-empirical methods have been developed (GORMONT [7]), (BEDDOES [8]), (GANGWANI [9]), (TRAN/PETOT [10]) to represent unsteady viscous effects, however, work is concentrated on pitch with some plunge extensions. The complex flow field of a rotor demands a more systematic modelling of viscous effects based on all degrees of freedom.

Hence, the DUHAMEL-integral procedure is used in the present investigation, to generalize the unsteady viscous effects. Just the coefficients of the approximate WAGNER function must be replaced. The result is an analytical correlation between the velocity and acceleration components and the re-

duced frequency.

Again the importance of a unified steady model is shown when unsteady viscous effects can be performed by just changing the steady maximum circulation points. The increment due to pitch motion can be written:

$$\Delta v_{zss+,-} = \frac{c}{2} \cdot \left\{ \dot{\Theta} \cdot \left[\frac{c_{us\Theta 1} \cdot k^2}{c_{us\Theta 2}{}^2 + k^2} \right] - \ddot{\Theta} \cdot \left[\frac{c_{us\Theta 1} \cdot c_{us\Theta 2}}{c_{us\Theta 2}{}^2 + k^2} \right] \right\}$$

Plunge motion results in:

$$\Delta v_{zss+,-} = \left\{ \dot{z} \cdot \left[\frac{c_{usz1} \cdot k^2}{c_{usz2}{}^2 + k^2} \right] - \ddot{z} \cdot \left[\frac{c_{usz1} \cdot c_{usz2}}{c_{usz2}{}^2 + k^2} \right] \right\}$$

This moving law for the maximum circulation point is applied for the lower and upper surface of a profile simultaneously but in opposite direction. Fig. 8 shows the positive circulation function dependent on different pitch rates.

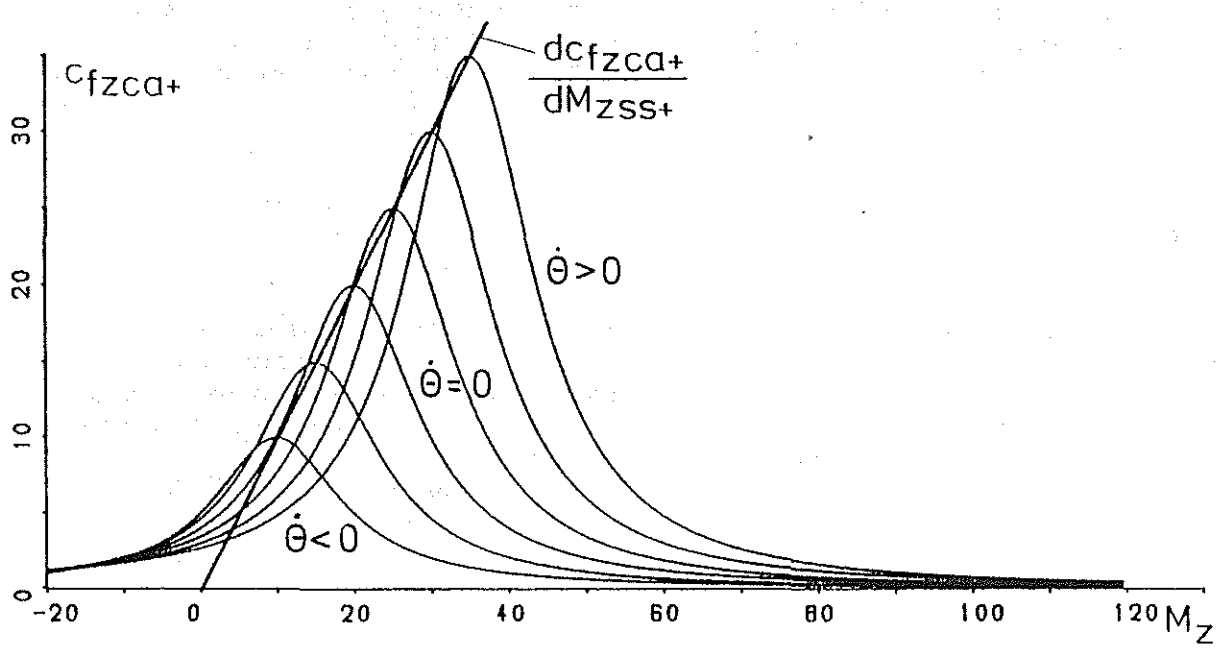

Fig. 8: Pitch rate influence on the positive circulation function

Each set of two empirical parameters of the pitch or plunge motion are identified by a nonlinear least square method based on measurement data. Acceleration and deceleration due to fore and aft motion influences the boundary layer in a similar way.

$$\Delta v_{zss+,-} = \left\{ \dot{x} \cdot \left[\frac{c_{usx1} \cdot k^2}{c_{usx2}{}^2 + k^2} \right] - \ddot{x} \cdot \left[\frac{c_{usx1} \cdot c_{usx2}}{c_{usx2}{}^2 + k^2} \right] \right\}$$

Experiments for identification of these empirical parameters have not yet been done, but are expected in the near future.

Finally the influence of the unsteady yaw must be considered. Due to limited space even the steady case was not presented within this paper. This special problem was investigated separately by LEISS[4] in great details.

4. Comparison With Measurements

As mentioned earlier, all empirical coefficients must be identified on measurement data or CFD results using a nonlinear least square method. One example is given in the appendix based on systematic measurements of the NACA 0012 profile.
A wide range of angle of attack and Mach number was performed (SCHEITLE/ WAGNER [11]). The presented plots illustrate the systematic superposition of flow types. The new normal and tangential force and pitching moment coefficients are shown. Because of the limited space an extensive demonstration of the steady and unsteady correlation with measurement data is impossible. For all aerodynamic coefficients the new model is within the measurement accuracy.

5. Conclusions

A new model was developed to unify the representation of rotor blade airloads. The model has no limitations in Mach number and angle of attack by the use of Mach number components. The superposition of different flow types gives a systematic structure of steady flow in the attached and separated flow regime. The new approach is valid for all aerodynamic coefficients in a generalized way. A relatively simple extension to unsteady effects is possible only on this steady model with physical content. The mathematical procedure of the Wagner function is introduced to the unsteady viscous effects. These effects are divided up into the degrees of freedom and modeled separately.
Even in simple analyses the present new model can be used without extensive work and computation time. The full analytical formulation of the model is the basis for analytical integration and the appropriate use of optimization techniques. Complex mechanism are represented in a relatively simple form within the accuracy of measurements.
In future the new model should be derived additional in the form of differential equations for application at aeroelastic analyses.

References

1. LEISS, U.: A Consistent Mathematical Model to Simulate Steady and Unsteady Rotor-Blade Aerodynamics, Proc. of the 10th European Rotorcraft Forum Paper No.7, Den Haag, The Netherlands, 1984

2. LEISS, U.: Semi-empirical Simulation of Steady and Unsteady Rotor Blade Aerodynamic Loading, Proc. of the International Conference on Rotorcraft Basic research, Raleigh, Research Triangle Park, 1985

3. LEISS, U./ WAGNER, S.: Analytische Darstellung der Stationären und Instationären Aerodynamischen Beiwerte Moderner Hubschrauberrotoren, DGLR-Nr. 85-114, DGLR-Jahrestagung, Bonn-Bad Godesberg, 1985

4. LEISS, U.: Unsteady Sweep - A Key to Simulation of Threedimensional Rotor Blade Airloads, Vertica, Vol.10, No.3/4, pp. 341-351, 1986

5. WAGNER, H: Über die Entstehung des dynamischen Auftriebs von Tragflügeln, Zeitschrift für angewandte Mathematik und Mechanik, Bd.5, Heft 1, Februar 1925

6. KÜSSNER, H.G.: Zusammenfassender Bericht über den Instationären Auftrieb von Flügeln, Luftfahrtforschung, Bd. 13, Nr.12, Dezember 1936

7. GORMONT, R.E.: A mathematical model of unsteady aerodynamics and radial flow for application to helicopter rotors, USAAMRDL Technical Report 72-67, 1972

8. BEDDOES, T.S.: Representation of Airfoil Behaviour, Vertica Vol.7, No.2, pp. 183-197, 1983

9. GANGWANI, S.T.: Synthesized Airfoil Data Method for Prediction of Dynamic Stall and Unsteady Airloads, 39th AHS Annual Forum, St. Louis, Missouri, Mai 1983

10. TRAN, C.T./ PETOT, D.: Semi-Empirical Model for the Dynamic Stall of Airfoils in View of the Application to the Calculation of a Helicopter Blade in Forward Flight, Vertica, Vol.5, pp. 35-53, 1981

11. SCHEITLE, H.: Meßreihen zur Bestimmung stationärer Profilbeiwerte der Profile NACA 0012, H1-Tb und H3-Tb, Institutsbericht 1987 am Institut für Luftfahrttechnik und Leichtbau der Universität der Bundeswehr München Bd.I,II

Acknowledgement

The paper is based on research work funded by the Bundesministerium für Forschung und Technologie BMFT (Ministry of Research and Technology).

Notation

a	sonic speed	M	moment
c	blade chord	t	blade thickness
c_i	aerodynamic cofficients	υ	viscosity
F	force	Θ	pitch angle
k	reduced frequency		

Subscripts:

a	attached	n	Newton
A	aerodynamic	ref	reference
am	apparent mass	ss	steady stall
b	bubble	t	transonic
ca	circulation attached	us	unsteady stall
cs	circulation separated	x,y,z	coordinate direction
f	force	+,-	in positive or negative coordinate direction
m	moment		

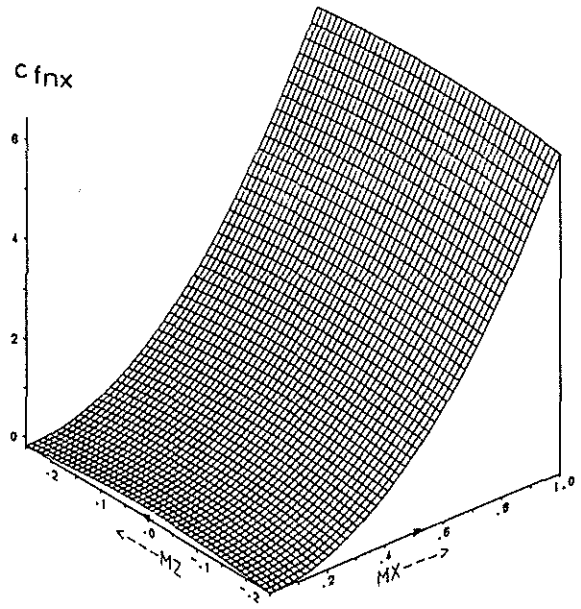
C_{fnx}
MZ
MX

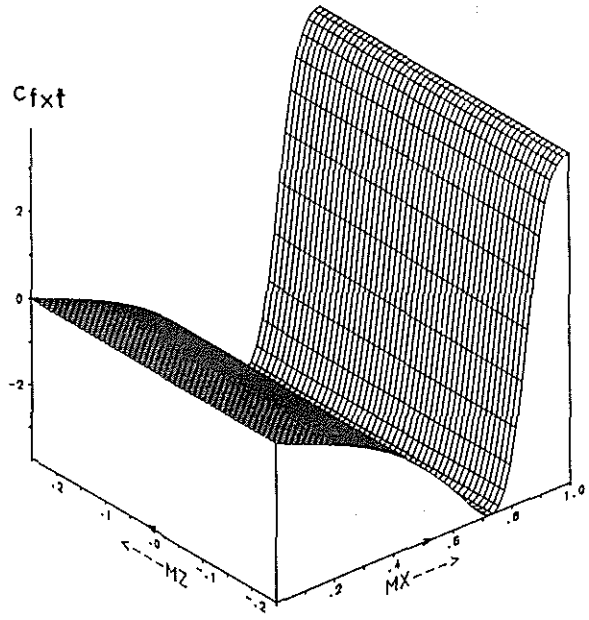
C_{fxt}
MZ
MX

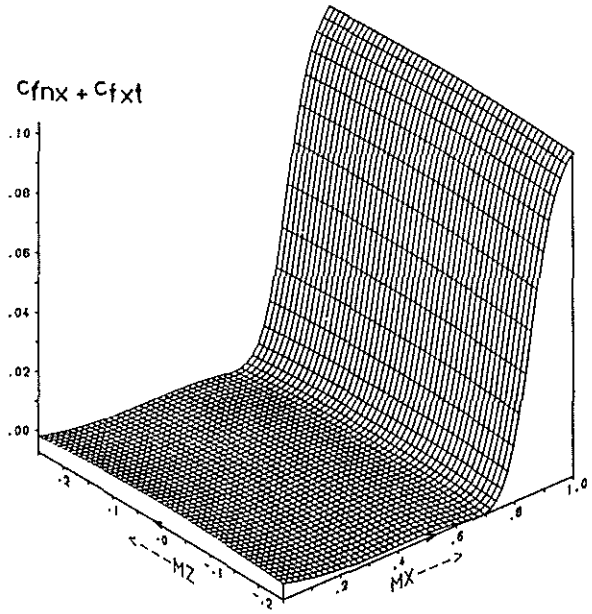
$C_{fnx} + C_{fxt}$
MZ
MX

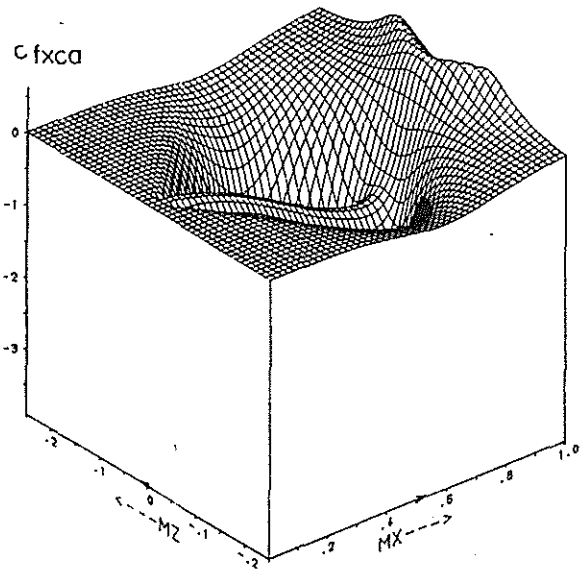
C_{fxca}
MZ
MX

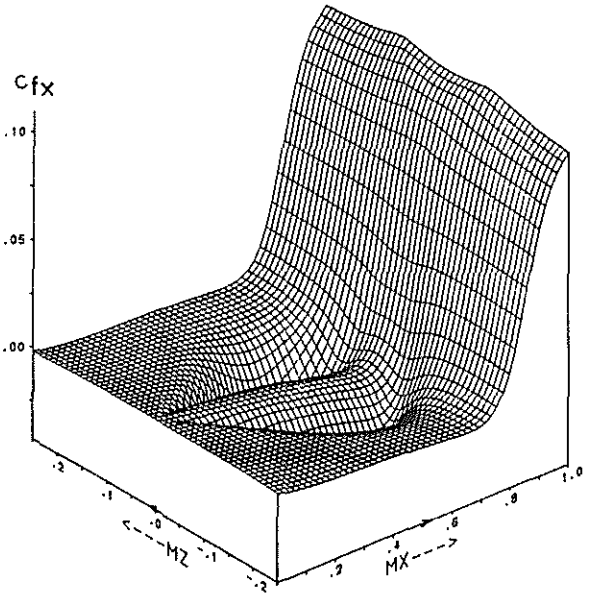
C_{fx}
MZ
MX

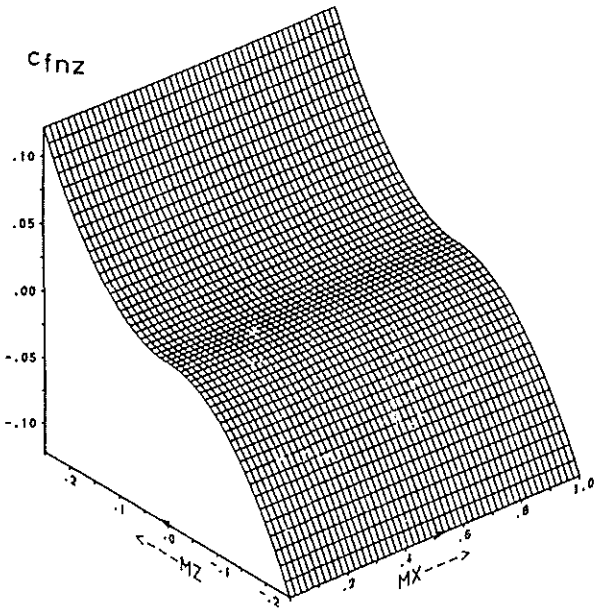
C_{fnz}
.10
.05
.00
-.05
-.10
<---MZ
MX--->
.2
.1
.0
-.1
-.2
.2
.4
.6
.8
1.0

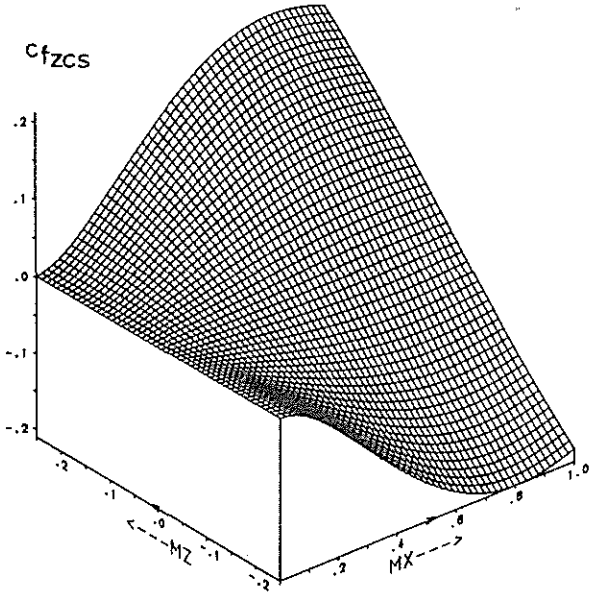
C_{fzcs}
.2
.1
.0
-.1
-.2
<---MZ
MX--->
.2
.4
.6
.8
1.0

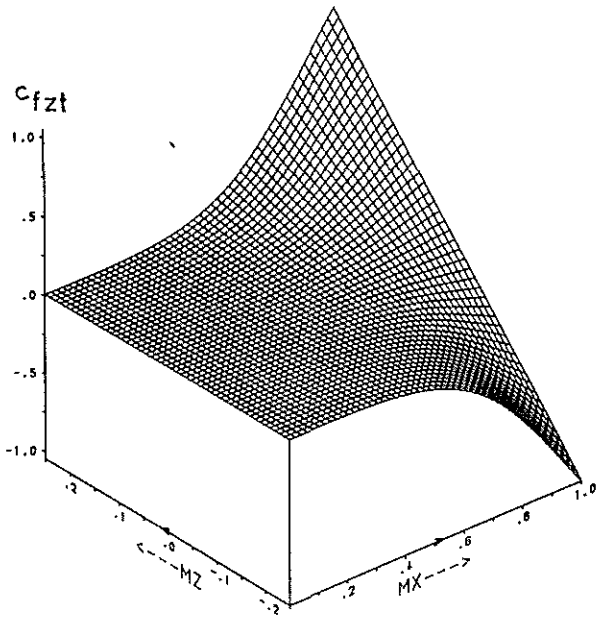
C_{fzt}
1.0
.5
.0
-.5
-1.0
<---MZ
MX--->
.2
.4
.6
.8
1.0

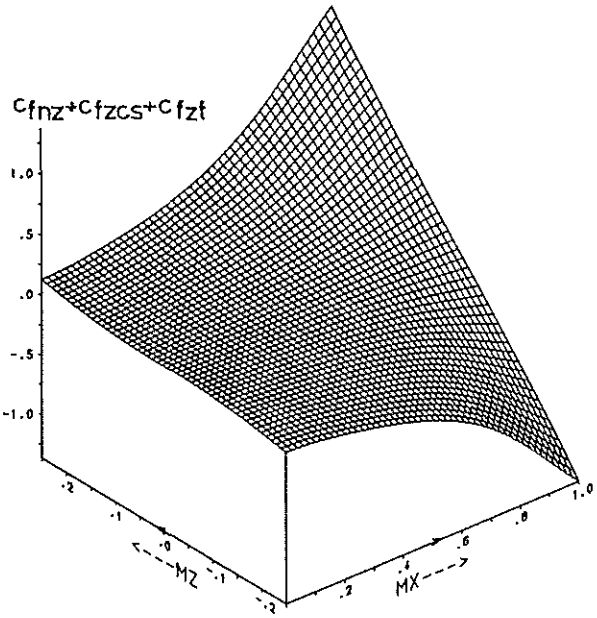
$C_{fnz}+C_{fzcs}+C_{fzt}$
1.0
.5
.0
-.5
-1.0
<---MZ
MX--->
.2
.4
.6
.8
1.0

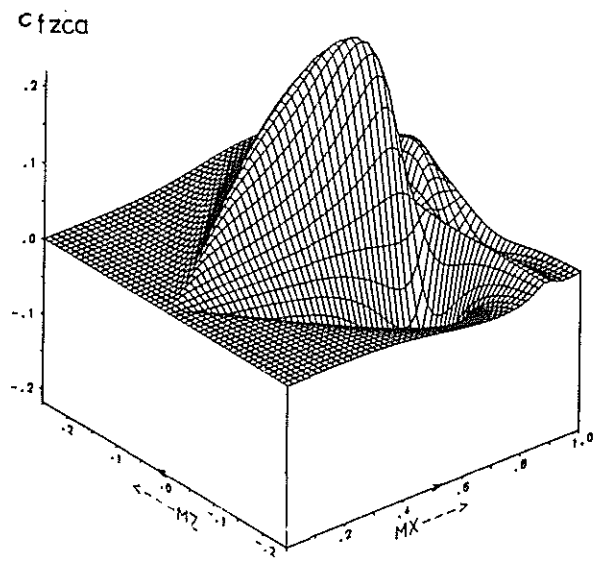
C_{fzca}
.2
.1
.0
-.1
-.2
<---MZ
MX--->
.2
.4
.6
.8
1.0

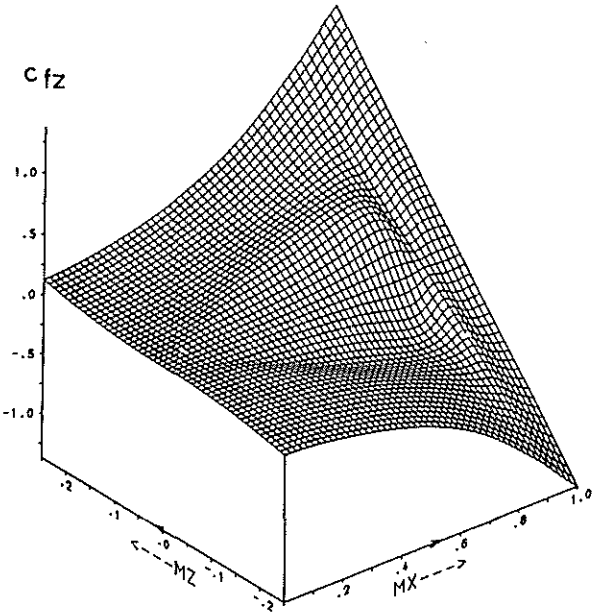
C_{fz}
1.0
.5
.0
-.5
-1.0
<---MZ
MX--->
.2
.4
.6
.8
1.0

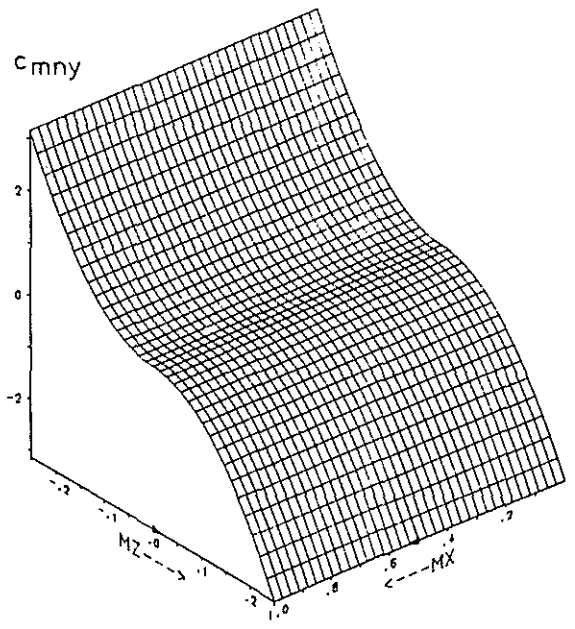
C_{mny}
MZ
MX

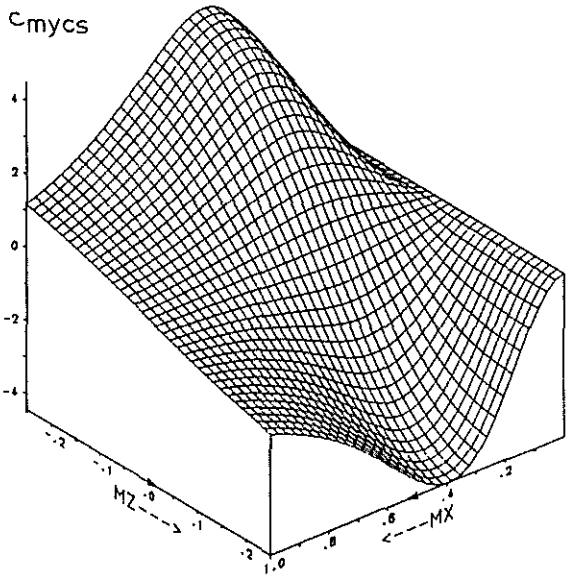
C_{mycs}
MZ
MX

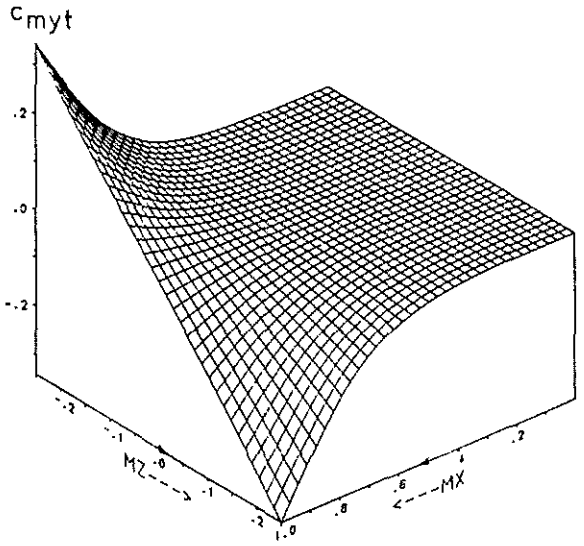
C_{myt}
MZ
MX

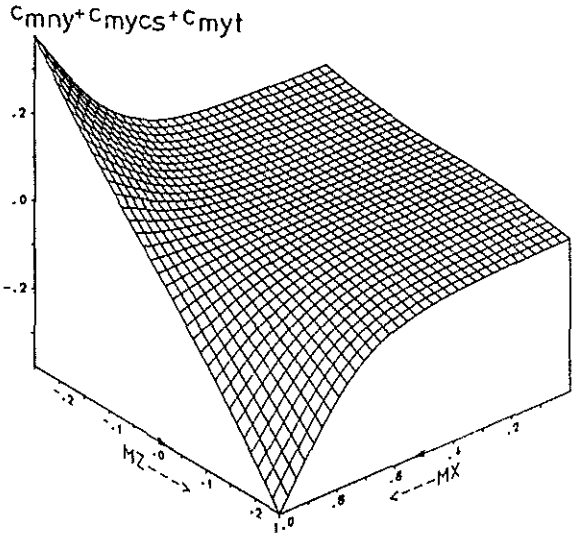
$C_{mny}+C_{mycs}+C_{myt}$
MZ
MX

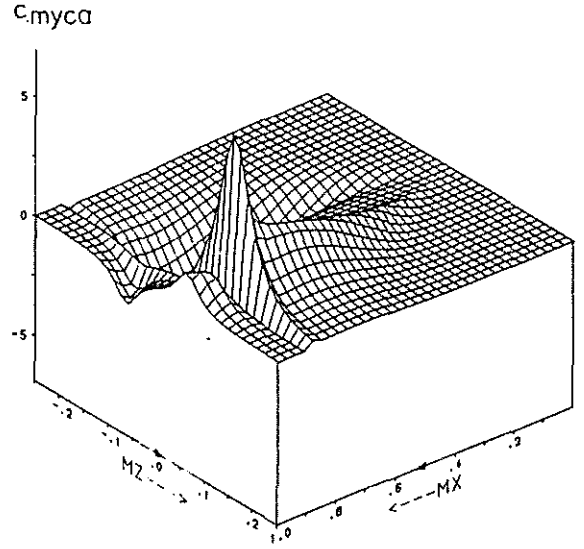
C_{myca}
MZ
MX

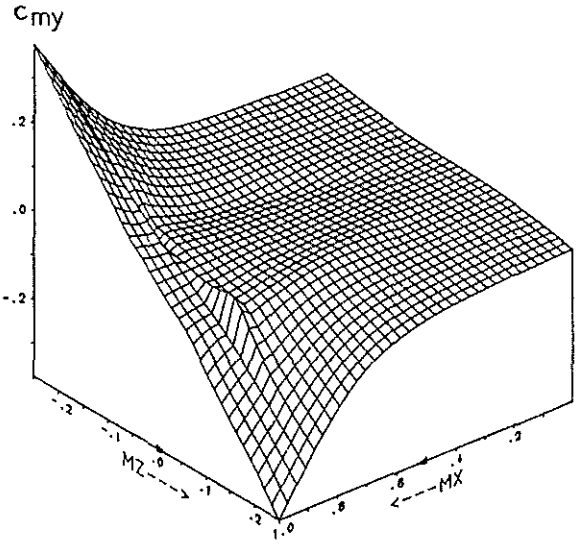
C_{my}
MZ
MX